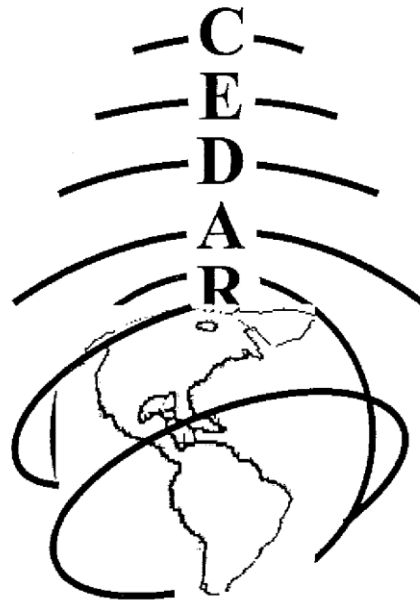




2009 CEDAR Workshop
Eldorado Hotel
Santa Fe, New Mexico, USA
June 28 – July 2, 2009



Monday CEDAR Poster Session Booklet
June 29, 2009



Table of Contents

Meteor Science other than Wind Observations

METR-01, Elizabeth Bass, Analysis of Simultaneous Meteor Observations With Specular and Incoherent Scatter Radars	1
METR-02, Elim Cheung, Comparison of Meteoroid Mass Estimates Using Multiple Instrument Observations	1
METR-03, Jonathan Sparks, The diurnal variability of the micrometeor altitude distribution and its relation to meteoroid astronomical and physical characteristics	1

Sprites

SPRT-01, Jingbo Li, Estimation of Charge in Sprites.....	2
SPRT-02, Mike Taylor, Airborne Image Measurements of Elves Over Southern Europe.....	2
SPRT-03, Lance Petersen, Comparison of Sprite-Halo Characteristics Imaged Over the USA and South America.....	2
SPRT-04, Gaopeng Lu, Lightning induction field above lightning strokes from impulse currents: one solution to sprites initiated by small charge moment changes.....	3
SPRT-05, Jeremy Riousset, Air Heating Associated with Transient Luminous Events.....	3
SPRT-06, Robert Marshall, Time-domain modeling of lightning-EMP induced ionospheric density perturbation and transient optical emissions.....	4

Instruments or Instruments or Techniques for Middle Atmospheric Observation

ITMA-01, Robert Marshall, PIPER: Photometric Imager for Precipitation of Electron Radiation.....	4
ITMA-02, Feng Han, Midlatitude D region variabilities detected by broadband VLF sferics.....	4
ITMA-03, Douglas Drob, Inversion of Infrasound Signals for Passive Atmospheric Remote Sensing.....	5
ITMA-04, Sean Harrell, Current status of the Faraday Filter-Based Spectrometer to Measure Sodium Nightglow D2/D1 Intensity Ratios	5
ITMA-05, Tom Slanger, CESAR (Compact Echelle Spectrograph for Aeronomical Research).....	6
ITMA-06, Matthew Hayman, ARCLITE Lidar for PMC Depolarization Measurements.....	6
ITMA-07, Steven Watchom, The Climate Monitoring Cubesat Mission (CM ²).....	6
ITMA-08, Tony Mangogna, 4-Channel Photometer for Atmospheric Gravity Wave Detection in Airglow Emissions	7
ITMA-09, Cody Vaudrin, A Multi-Channel FPGA Based High Speed Digital Receiver: Development, Applications and Data Processing.....	7

Mesosphere and Lower Thermosphere Lidar Studies

MLTL-01, Zhangjun Wang, Design and Development of LabVIEW-Based Novel Software for MRI Lidar System	7
MLTL-02, John Smith, Robust seed laser frequency stabilization for narrowband Doppler lidars	8
MLTL-03, Chiao-Yao She, Recent advances in midlatitude long-term temperature variations deduced from Na lidar observations with brief summary of tidal and mean temperature/wind climatology.....	8
MLTL-04, Brita Irving, Rayleigh Lidar Observations of the Arctic Stratosphere and Mesosphere during the International Polar Year	9
MLTL-05, Brentha Thurairajah, Gravity Wave Activity in the Arctic Middle Atmosphere: Rayleigh Lidar Measurements and Analysis.....	9
MLTL-06, Xianghui Xue, Possible Relations between Meteors, Enhanced Electric Density Layers and Sporadic Sodium Layers.....	9
MLTL-07, Jia Yue, Convective and dynamic stabilities, large wind shears in the mesopause observed by Na lidar at Fort Collins, CO (41°N, 105°W).....	9
MLTL-08, Wentao Huang, Simultaneous Wind and Temperature Measurements from Lower to Upper Atmosphere.....	10

Mesosphere and Lower Thermosphere Gravity Waves

MLTG-01, Chad Carlson, High frequency gravity wave observations at UAO	10
MLTG-02, Amal Chandran, Gravity wave effects on polar mesospheric clouds: A comparison of numerical simulations with AIM observations.....	11
MLTG-03, Durga Kafle, Mesospheric Atmospheric Gravity Waves Observed by Rayleigh-Scatter Lidar	11

MLTG-04, Tao Li, Seasonal and inter-annual variability of gravity wave activity revealed from long-term lidar observations over Mauna Loa Observatory, Hawaii	12
MLTG-05, Jonathan Pugmire, Intra-Annual Comparison of Mesospheric Gravity Waves Over Halley and Rothera Stations, Antarctica.....	12
MLTG-06, Deepak Simkhada, Ripple Climatology Observed in the Mesopause Region over Maui, Hawaii	13
MLTG-07, Camille Smith, Mesospheric Gravity Waves Over Equatorial Brazil.....	13
MLTG-08, Qian Wu, Tri-station Observation of Polar Mesospheric 10-hr Inertio Gravity Wave	13
MLTG-09, Robert Thacker-Dey, Investigations of wave-induced secular variations of exothermic heating in the MLT region	14
MLTG-10, Roger Hale Varney, Case Study of an Inertia-Gravity Wave in the Mesosphere over Alaska with the Poker Flat Incoherent Scatter Radar.....	14
MLTG-11, Xun Zhu, A Spectral Parameterization of Drag, Heating and Eddy Diffusion for a Three-Dimensional Mean Flow Induced by Breaking Gravity Waves	14
MLTG-12, Jonathan Snively, Observation and modeling of OH airglow temperature and intensity perturbations by mesospheric gravity waves.....	15
MLTG-13, José Valentin Bageston – presented by Igo Paulino Mesospheric Front in a Doppler Duct Observed over Ferraz Station, Antarctica (62°S)	15
MLTG-14, Igo Paulino, Estimation of large scale gravity wave parameters using airglow images	15

Mesosphere and Lower Thermosphere Other Tidal or Planetary Waves

MLTT-01, Loren Chang, Influence of an Ultra Fast Kelvin Wave on the Migrating Diurnal Tide.....	16
MLTT-02, Jonathan Friedman, Longitude Variations of the Solar Semidiurnal Tides in the Mesosphere and Lower Thermosphere at Low Latitudes Observed from Ground and Space	16
MLTT-03, Xian Lu , The Seasonal and Intraseasonal Variation of the Diurnal Tide in the Mesosphere and Lower Thermosphere Observed by Meteor Radar over Maui, HI (20.7o N, 156.3o W).....	16
MLTT-04, Tao Yuan, A Collaborative Study on Temperature Diurnal Tide in the midlatitude Mesopause region by Na lidar (41°N, 105°W) and TIMED/SABER	17
MLTT-05, Jung Soo Kim, Investigation of Thermospheric Density Modeling on a Diurnal Time Scale	17
MLTT-06, Pruthvish Bena Patel, Observations of 6- and 8- hour period waves at the South Pole	18
MLTT-07, Bob Stockwell, Local Spectral Analysis of very long Radar Wind Time Series	18
MLTT-08, Bob Stockwell, Principal Harmonic Analysis of tidal signals in radar winds.....	18

Mesosphere or Lower Thermosphere General Studies

MLTS-01, Jose Fernandez, Quiet-Nighttime TIMED/SABER NO+(v) VER Data Characterization at E-region Altitudes	19
MLTS-02, Pedrina Terra Santos, Simultaneous OII 7320 Å Line Width and Incoherent Scatter Radar O+ Temperatures Measured at Arecibo	19
MLTS-03, Sebastien de Larquier, Development of efficient finite-difference time-domain models of infrasound propagation in a realistic atmosphere	19
MLTS-04, Jonathan Fentzke, Meteoric smoke particle properties derived using dual-beam Arecibo UHF observations of D-region spectra during different seasons.....	20
MLTS-05, Zhenhua Li, An investigation of the impacts of temperature and large-scale circulation on OH airglow using SABER data	20
MLTS-06, Tyler David Scott, Rocket Observations of Lower Thermospheric Winds at High Latitudes During Active Conditions.....	20
MLTS-07, Padma Thirukoveluri, Planning and simulating observations for a sounding rocket experiment Measuring thermospheric nitric oxide (NO) in the polar night by stellar occultation.....	21
MLTS-08, Chihoko Yamashita, Gravity wave impacts on the atmospheric coupling from the MLT region to the stratosphere during stratospheric sudden warming with TIME-GCM	21
MLTS-09, Katelynn Greer, Baroclinic Conditions and Anomalous Temperature Excursions of the Arctic Winter Middle Atmosphere: Discovery of Separated Mesopauses	21
MLTS-10, Jaimy Tomlinson, Correlation of Mesospheric Polar Cloud Observational Data for the Northern Hemisphere in 2007	22

Meteor Science other than Wind Observations

METR-01 Analysis of Simultaneous Meteor Observations with Specular and Incoherent Scatter Radars - by Elizabeth Bass

Status of First Author: Student IN poster competition PhD

Authors: Elizabeth Bass, Meers Oppenheim, Glenn Sugar, Jorge Chau, Freddy Galindo

Abstract: For over 60 years, specular radars have used meteor detections to determine meteoroid properties and to estimate Mesosphere and lower Thermosphere (MLT) winds, while large incoherent scatter radars detected meteors but have only made use of the information in the past decade. However, no previous experiment has successfully measured the same meteor with both instrument types. In February 2008, concurrent specular and non-specular meteor observations were conducted using the 50 MHz incoherent scatter radar at the Jicamarca Radio Observatory (11.95° S, 76.87° W) and the specular radar at Paracas (13.85° S, 76.25° W). Three meteoroids were detected with both instruments, only one of which returned a high SNR in both receivers. In this poster, we compare the timing of the signals as well as the evolution of the signal strength; both have a very short rise time, but the specular and non-specular signal decay rates are noticeably different. In addition, we calculate wind speeds from both the JRO and the Paracas data. While wind speeds do not correspond exactly, the variation is consistent with the wind profiles around 100 km by Oppenheim et al. (2009).

METR-02 Comparison of Meteoroid Mass Estimates Using Multiple Instrument Observations by Elim Cheung

Status of First Author: Student IN poster competition Undergraduate

Authors: Elim Cheung, Elizabeth Bass, Dr. Meers Oppenheim, David Nero, Dr. T. Sato and Dr. T. Nakamura

Abstract: Every year, billions of meteors disintegrate in the Earth's upper atmosphere. An accurate measurement of meteoroid mass will enable us to better understand the effects of metals in our Earth's atmosphere, the risk of meteoroid impact on satellites, and the nature of the outer solar system. Using a data set collected at the MU radar observatory in Japan, this study compares the mass estimates determined by three different techniques: the meteoroid deceleration approach, the RCS scattering method developed by Close et al. (2004), and the optical method used by Nishimura et al. (2001). Among the 15 meteoroids observed by both instruments, only one of the meteoroids has all three masses with the same order of magnitude. In general, optical masses and RCS scattering masses are similar to within an order of magnitude. In contrast, deceleration masses are typically smaller than the other two. In this poster, we examine the inconsistency among the different methods and suggest ways to improve the calculations.

METR-03 The diurnal variability of the micrometeor altitude distribution and its relation to meteoroid astronomical and physical characteristics - by Jonathan Sparks

Status of First Author: Student IN poster competition Undergraduate

Authors: Jonathan Sparks, sparksj@colorado.edu; Diego Janches, diego@cora.nwra.com

Abstract: We present a study of the diurnal behavior of the observed meteor altitude distribution at different seasons and latitudes. This study utilizes head-echo observations collected with the 430 MHz Arecibo radar in Puerto Rico and the 450 MHz Poker Flat Incoherent Scatter Radar (PFISR) in Alaska. The meteor altitude distribution provides an indication of where the meteoric mass deposition occurs in the mesosphere and lower thermosphere (MLT). This can be utilized to model the input of metallic constituents into the MLT and accurately understand the chemistry of this region. We show that the observed altitude distributions have distinct variability at each location: at high latitudes there is a weak diurnal and strong seasonal variability while at tropical latitudes the opposite behavior is observed. We explain these results by correlating them with the astronomical and physical properties of the meteoric flux. At different geographical locations the meteoroid entry angles vary differently with time of the day and season potentially filtering the mass/velocity particle populations and producing the distinct observed results.

Sprites

SPRT-01 Estimation of Charge in Sprites - by Jingbo Li

Status of First Author: Student IN poster competition PhD

Authors: Jingbo Li, j1108@ee.duke.edu; Steven Cummer, cummer@ee.duke.edu

Abstract: Low frequency radio emission indicates that substantial electric current flows inside sprites. This charge motion, with unknown location and distribution, is related with the detail internal microphysics of sprite development that is connected to the effects sprites create in the mesosphere. Models developed based on electrical and chemical processes can predict the distribution of charges in sprites. However, it is hard to measure the electric fields and charge distribution inside sprites due to their small spatial scale, short temporal scale, and inaccessibility. In this work, we attempt to infer the charge distribution in sprites by combining measurements of lightning radiated magnetic fields, high speed sprite images recorded at 1,000 – 10,000 fps, and numerical simulations. A 2-D FDTD model is used to estimate the lightning-generated background electric fields in mesosphere through measurements of lightning source current waveform. Assuming sprite streamers propagate in the direction of local electric field, we combine this background electric field and streamer propagation direction measured from high speed images to estimate the total ambient electric field at streamer head locations, which is caused by both sprite-producing lightning and adjacent sprite streamers. The charge distribution in different sprite features can be inferred from this total electric field. We also compare this estimated charge distribution with model predicted values. Our result is a step toward constraining the detailed physical and chemical models that can predict the impact of sprites on the mesosphere.

SPRT-02 Airborne Image Measurements of Elves over Southern Europe - by Mike Taylor

Status of First Author: Non-student

Authors: M. J. Taylor, P.-D. Pautet, L.C. Gardner, C. Price, S. Abe, H.Yano, P. Jenniskens

Abstract: Elves appear as rapidly expanding horizontal disks of light at the base of the night-time ionosphere due to the absorption of electromagnetic pulse (EMP) energy generated by powerful cloud-to-ground (CG) lightning discharges (with peak currents typically >80 kA). They were first postulated in 1993 to explain unusual transient limb “brightenings” observed at mesospheric airglow heights (~90 km) from the Space Shuttle, and subsequently were measured using ground-based high-speed mapping array photometers (Fukunishi et al., 1996). Elves occur within a few hundred μ s of the parent lightning discharge, well ahead of the onset of sprite emissions. Modeling and recent satellite measurements have shown that they can attain a diameter of a few to several hundred kilometers and usually exhibit a characteristic “donut shape” with a dark central hole (for a near vertical CG). To date, most elve studies have been performed using specialized narrow-field photometer arrays (e.g. Barrington-Leigh et al., 2001) that are capable of measuring their temporal evolution during their very short lifetimes (<0.5 ms), but not their integrated two-dimensional structure. In this poster we report an exceptional set of airborne measurements of elves (and sprites) imaged over southern Europe using intensified video cameras operating at standard video frame rates (30 fps). The serendipitous observations were made during the NASA Leonid-MAC Airborne Campaign on the night of 17/18 November, 1999 over a period of ~1 hour close to the peak of the Leonids meteor storm. These observations predate more recent satellite studies, and provide important new information on the occurrence, scale-sizes, polarity and association of 18 distinct elves with two isolated, early winter-time storms over the Dalmatian coast.

SPRT-03 Comparison of Sprite-Halo Characteristics Imaged Over the USA and South America by Lance W. Petersen

Status of First Author: Student IN poster competition Undergraduate

Authors: Lance W. Petersen; M. J. Taylor; M. A. Bailey; J. Hayes; P-D Pautet; S. A. Cummer

Abstract: Sprites and Halos are prominent members of an extraordinary family of Transient Luminous Events (TLE's)_that have been discovered over the past 20 years. Halos are short-lived (few millisecond) diffuse optical emissions

that appear as horizontal bright disks suspended briefly above distant thunderstorms. They frequently (but not always) precede the formation of a vertically structured sprite. Although easy to capture using intensified video cameras operating at standard rates (30 frames per second), reports of halos are relatively few and indicate a limited height range centered around approximately 80 km with optical diameters up to about 100 km. Unlike sprite events, which occur almost exclusively in association with large positive cloud-to-ground lightning discharges, halos have recently been observed from satellite in association with both positive and negative discharges. This poster presents an initial comparison of the optical and electrical properties (where known) of a large number of halos and sprite-halos imaged over the U.S. Great Plains and over Northern Argentina in South America. Our goal is to improve current knowledge of their characteristics and variability.

SPRT-04 Lightning induction field above lightning strokes from impulse currents: one solution to sprites initiated by small charge moment changes - by Gaopeng Lu

Status of First Author: Non-student

Authors: Steven A. Cummer, Electrical and Computer Engineering Department, Duke University, cummer@ee.duke.edu; Jeremy Norman Thomas, Bard College/University of Washington/NWRA, jnt@u.washington.edu

Abstract: Lightning induction field above positive cloud-to-ground strokes is examined for impulse currents of varying durations and the result is compared with the electrostatic field that plays a major role in producing sprites at mesospheric altitudes. It is shown that the induction field makes a significant contribution when the impulse current lasts ~ 1 ms or less. For positive strokes with high peak currents (e.g., >100 kA) and short durations (e.g., ~ 0.5 ms), the induction field might be the dominant term that initiates sprites with short post-stroke delays and small charge moment changes. A comprehensive criterion that assesses the capability of a lightning stroke in initiating sprites should include both charge moment change and current moment change, evaluating the electrostatic and induction component in lightning electric fields, respectively.

SPRT-05 Air Heating Associated with Transient Luminous Events - by Jeremy A. Rioussset

Status of First Author: Student NOT in poster competition PhD

Authors: Jeremy A. Rioussset, CSSL Laboratory, Penn State University, University Park, Pennsylvania 16802, USA (rioussset@psu.edu); Victor P. Pasko, CSSL Laboratory, Penn State University, University Park, Pennsylvania 16802, USA (pasko@psu.edu); Anne Bourdon, EM2C UPR 288 Ecole Centrale Paris, Grande voie des vignes, 92295 Châtenay-Malabry Cedex, France (anne.bourdon@em2c.ecp.fr)

Abstract: The understanding of ambient gas heating processes initiated by needle-shaped filaments of ionization, called streamers, embedded in originally cold air (near room temperature) represents a long standing problem, which is of interest for studies of long laboratory sparks and natural lightning discharges [e.g., Gallimberti et al., C. R. Physique, 3, 1335, 2002]. The observed phenomenology of a subset of the recently observed transient luminous events in the middle atmosphere, which originate from thundercloud tops [e.g. Wescott et al., JGR, 106, 21549, 2001; Pasko et al., Nature, 416, 152, 2002; Su et al., Nature, 423, 974, 2003; Krehbiel et al., Nature Geoscience, 1, 233, 2008], indicate that these events may be related to conventional lightning leader processes and therefore are associated with significant heating of the air in the regions of atmosphere through which they propagate [Pasko and George, JGR, 107, 1458, 2002]. Many of the small-scale features observed in sprites at higher altitudes [e.g., Stenbaek-Nielsen et al., GRL, 104, L11105, 2007, and references therein] can be interpreted in terms of corona streamers, which, after appropriate scaling with air density, are fully analogous to those, which initiate spark discharges in relatively short (several cm) gaps at near ground pressure [Liu et al., JGR, 114, A00E03, 2009, and references therein] and which constitute building blocks of streamer zones of conventional lightning leaders in long gaps [Gallimberti et al., 2002]. The recent reports of infrasound bursts originating from 60-80 km altitudes in sprites, with durations consistent with the optical widths of the sprites [e.g., Farges, in Lightning: Principles, Instruments and Applications, p. 417, Betz et al., (eds.), Springer, 2009], provide an additional motivation for studies of the heating of the ambient air and associated chemical effects caused by streamers in transient luminous events. In this talk we will discuss scaling properties of physical processes involved in the air heating in streamer channels as a function of air pressure and will report the most recent results from a model developed for investigation of effective time scales of air heating in streamer channels. The model explicitly includes energy input in fast heating, vibrational excitation of nitrogen molecules, the vibrational-translational relaxation processes, and accounts for the effects of gains in electron energy in

collisions with vibrationally excited nitrogen molecules on the rate constants of ionization and dissociative attachment processes [Belinov and Naidis, J. Phys. D: Appl. Phys., 36, 1834, 2003, and references therein]. We will discuss performance of different models proposed in recent literature for positive ion chemistry, including O₂⁺, O₄⁺ and O₂+N₂ ions.

SPRT-06 Time-domain modeling of lightning-EMP induced ionospheric density perturbation and transient optical emissions - by Robert Andrew Marshall

Status of First Author: Student IN poster competition PhD

Authors: Robert A. Marshall, Umran S. Inan, Robert T. Newsome

Abstract: Elves are transient glows in the D-region ionosphere caused by the electromagnetic pulse (EMP) from intense lightning discharges. Recent observations have shown that a) the Earth's magnetic field may affect elve observations, and b) elves may be produced by horizontal in-cloud (IC) lightning. In this work we present results of a 3D finite-difference time-domain (FDTD) model of the lightning EMP-ionosphere interaction, taking into account the Earth's magnetic field, and allowing the use of an arbitrarily-oriented source current at any altitude. We include cold plasma effects and nonlinear effects such as heating, ionization and optical emissions, in order to predict the effects of the lightning EMP in the ionosphere and the shape and time signature of observed elves. We show that the Earth's magnetic field creates an observable asymmetry in the elve signature, which may be observable in some elve images. Furthermore, we show that in-cloud lightning, particularly bursts of in-cloud discharges, can create a significant density enhancement in the D-region ionosphere, as well as a potentially observable optical signature. These signatures are compared with recent camera and photometric images from the PIPER instrument.

Instruments or Instruments or Techniques for Middle Atmospheric Observation

ITMA-01 PIPER: Photometric Imager for Precipitation of Electron Radiation
by Robert Andrew Marshall

Status of First Author: Student NOT in poster competition PhD

Authors: Robert A. Marshall, Umran S. Inan

Abstract: A new optical instrument has been developed that captures a low-light 2-D scene at high speed and high sensitivity using 1-D photomultiplier tube arrays. The PMT arrays are orthogonally aligned, and using a coaligned video-speed imager, fast images can be reconstructed using matrix inversion techniques. The PIPER instrument can be used to make measurements of optical signatures of energetic electron precipitation induced by discrete waves (e.g., lightning discharges and very-low-frequency transmitter pulses), as well as measurements of high-speed, high-altitude glow discharges in the upper atmosphere known as sprites, halos, and elves. In this paper, we present the instrument design and capabilities, as well as some results of sprites and elves. The PIPER instrument has recently shown that elves are far more common than sprites, where previously, due to the limited sensitivity of cameras, elves were far more rarely observed.

ITMA-02 Midlatitude D region variabilities detected by broadband VLF sferics
by Feng Han

Status of First Author: Student IN poster competition PhD

Authors: Feng Han

Abstract: Broadband VLF sensors located near Duke University have been operating with the aim of studying the midlatitude ionospheric D region variability through measuring the sferic signals launched by the lightning and propagating in the Earth-Ionosphere waveguide. Significant temporal variability of the nighttime D region is well known, and we aim to study the time scales and possible sources of those variabilities in this work. We analyzed sferic data of July and August, 2005 recorded by our sensors through comparing measured sferic spectra to model results and extracted the two-parameter exponential electron density profile for each measurement. We found that the D region electron density varies

from night to night and hour to hour in the same night. The possible reasons including lightning induced electron precipitation generating secondary ionization and direct energy coupling between lightning and lower ionosphere are also analyzed in the context of those measurements.

ITMA-03 Inversion of Infrasound Signals for Passive Atmospheric Remote Sensing by Douglas P. Drob

Status of First Author: Non-student

Authors: Douglas P. Drob (1), Robert R. Meier (2), J. Michael Picone (2), Milton A. Garcés (3)

(1) Space Sciences Division, U.S. Naval Research Laboratory, 4555 Overlook Avenue, Washington, DC 20375.

(2) Department of Physics and Astronomy, George Mason University, MS 3F3, Fairfax VA 22030.

(3) Infrasound Laboratory, HIGP, SOEST, University of Hawaii, Manoa, 73-4460 Queen Kaahumanu Hwy., #119, Kailua-Kona, HI 96740-2638.

Abstract: During the past few years, significant progress has been made in our understanding of atmospheric propagation of infrasound signals from both natural and man-made impulsive events. In this paper, we review this progress within the framework of the early history of infrasound remote sensing, including basic geophysical remote sensing theory and linear acoustic wave propagation.

We believe that the state-of-the-art in infrasound propagation research has advanced sufficiently that the opportunity is now at hand to turn the problem around and use detections of infrasound to improve our knowledge of upper atmospheric winds and temperatures. Accordingly, we employ discrete inverse theory, a concept developed by the seismographic and oceanographic communities, to infer winds and temperatures from infrasound observations. We demonstrate the methodology through application to an extensive time series of synthetic data generated using an atmospheric model as the “truth”.

The results of several illustrative numerical experiments carried out with an existing infrasound network show that with selected assumptions, infrasound signals from a single impulsive event can be inverted to provide quantitative information on the state of the middle- and upper atmosphere. We conclude that this approach to infrasound signal inversion is an important step forward in atmospheric remote sensing and we propose several ideas for future directions.

ITMA-04 Current status of the Faraday Filter-Based Spectrometer to Measure Sodium Nightglow D2/D1 Intensity Ratios - by Sean D. Harrell

Status of First Author: Student IN poster competition PhD

Authors: Sean D. Harrell, Chiao-Yao She, David A. Krueger, Tao Yuan
Colorado State University Department of Physics

Abstract: The Chapman mechanism (1939) offers the accepted chemical pathway for the production of excited states of mesospheric sodium, leading to nightglow at two wavelengths: D2 (589.158 nm) and D1 (589.756 nm). While the Chapman mechanism leaves open the possibility that the intensity ratio of the two transitions may vary due to the chemical reaction involving atomic oxygen, early observations by Sipler and Biondi (1978) yielded the value of two within experimental error. Recent work by Slinger et al. (2005), however, showed that not only does the intensity ratio vary, but its value is related to the concentration ratio of atomic oxygen [O] to molecular oxygen [O₂]. They proposed a modification of the Chapman mechanism involving two competing chemical pathways for sodium production to account for the observed variation.

This poster describes the current status of the compact, Faraday filter-based spectrometer to measure the D2/D1 intensity ratio of the nightglow. The novelty of this method also permits determination of the fractional contributions of the two chemical pathways to test the validity of the modified Chapman mechanism for Na chemistry, as well as to infer information about [O]/[O₂]. Since the delineation between the two chemical pathways requires a spectral resolution of 0.0002 nm, this is not possible with any other existing instrument. With this spectrometer deployed at the Colorado State University sodium lidar facility (41°N, 105°W), we expect to be able to measure short-term variations of the sodium nightglow intensity ratio and the chemical pathway fraction, from which [O]/[O₂] can be inferred. These observations may

yield new insights into mesospheric chemistry involving atomic and molecular oxygen, which play a key role in upper atmospheric chemistry and dynamics.

ITMA-05 CESAR (Compact Echelle Spectrograph for Aeronomical Research) - by Tom Slanger

Status of First Author: Non-student

Authors: Tom G. Slanger, Martin Grill, Vineeth Chandrasekharan Nair, Elizabeth Kendall
SRI International, Menlo Park, CA 94025, tom.slanger@sri.com

Abstract: The CESAR instrument is being constructed at SRI International with funds from the NSF MRI program. In this poster, we show various stages of the design. The camera design and optics assembly are being produced by INO (Quebec City), the detector by Spectral Instruments (Tucson, AZ).

The concept of CESAR is to extend the spectroscopic investigations we have carried out with the aid of the sky spectra of the large astronomical observatories (Keck I, Keck II, and the Very Large Telescope in Chile). The disadvantages of using sky spectra is that 1) they are from a fixed equatorial site, 2) we only obtain archived data, and 3) we have no control over observing conditions (direction and data accumulation times). With CESAR, the intention is to initially site the instrument at high latitude (Poker Flat Rocket Range) and study aurora and nightglow at high resolution, with control over pointing, and in conjunction with other investigators using their own instruments. Collaboration with facilities such as AMISR and HAARP are anticipated.

We will show results of optical modeling, the camera and detector assembly, and provide some answers relating to questionnaires we have sent out.

*The initial overall design is from Lyle Broadfoot. The preliminary optical design was made by Jean Lacoursière, currently at the Dominion Observatory in Victoria, British Columbia.

ITMA-06 ARCLITE Lidar for PMC Depolarization Measurements - by Matthew M. Hayman

Status of First Author: Student IN poster competition PhD

Authors: Matthew M. Hayman, Jeffrey P. Thayer, J.D. Vance

Abstract: PMC particles are small compared to the 532 nm wavelength used to probe them in the ARCLITE lidar. Because they are on the boundary of the Rayleigh/Mie scattering regions, depolarization will increase monotonically with increased asphericity. However, the small particle size also imposes a system requirement that the lidar be able to distinguish very small depolarizations. To meet this requirement, polarization cross talk must be minimized in the system, and the summer Arctic's persistent solar background reduced. In this work, we discuss our polarization rejection method used to reduce solar background and our recent development in polarization hardware compensation that will improve the ARCLITE lidar's performance as a PMC depolarization lidar through reduction in polarization channel cross talk.

ITMA-07 The Climate Monitoring Cubesat Mission (CM²) - by Steven Watchorn

Status of First Author: Non-student

Authors: Steven Watchorn, Rick Doe, John Noto, Karl Van Dyk

Abstract: The development of a new hyperspectral imager (HSI) for a Cubesat payload will be discussed. The HSI is based on the monolithic, field-widened Spatial Heterodyne Spectrometer (SHS), and will be designed to observe mesospheric and mesopause temperatures in the oxygen A-band.

A full-scale model of the payload -- including input and output optics and detector -- has been constructed by SRI and Scientific Solutions, and confirmed to fit in a 1.5-U Cubesat payload.

The science of the mission, instrument parameters, and optical and physical modeling of the payload will be presented.

ITMA-08 4-Channel Photometer for Atmospheric Gravity Wave Detection in Airglow Emissions by Tony Mangogna

Status of First Author: Student IN poster competition Masters

Authors: Anthony Mangogna (mangogni@illinois.edu), Gary Swenson (swenson1@illinois.edu), Alan Liu (liuzr@illinois.edu), Chad Carlson (ccarlso2@illinois.edu)

Abstract: At altitudes between 80-110 km in the Earth's atmosphere, chemiluminescent processes referred to as airglow emissions occur in strata. Perturbations in the airglow can indicate the presence of atmospheric gravity waves. These waves are useful for understanding the dynamics of the upper atmosphere and transport of momentum from the lower atmosphere to the mesosphere. Wave characteristics can be determined by studying multiple airglow layers simultaneously. For the purpose of measuring changes in the volume emission rate of an airglow layer, a 4-channel photometer was built. The 4-channel photometer has three channels dedicated to gathering airglow signal from three different layers: OH, O₂, and green line. The fourth channel gathers signal from the background, which is used to remove unwanted signal from the airglow channels. A unique method is presented for background removal from the airglow channels. Phase comparisons are made between each corrected airglow signal to determine vertical wavelength. Simultaneous measurements were made using the 4-channel photometer and an all-sky imager to perform relative wind measurements.

ITMA-09 A Multi-Channel FPGA Based High Speed Digital Receiver: Development, Applications and Data Processing - by Cody Vaudrin

Status of First Author: Student IN poster competition Masters

Authors: Cody Vaudrin, Scott Palo

Abstract: A new instrument for meteor radar data acquisition is defined by a minimal RF front-end followed by an analog-to-digital converter (ADC) controlled by a reconfigurable logic device (FPGA). Received data is eventually transferred to a host PC for storage and post-processing via a standard communications protocol (in this case USB 2.0). Design and implementation of the current FPGA based digital receiver is discussed. Main hardware components and electrical interfaces are outlined including the Xilinx Virtex 5 FPGA, Analog Devices 9252 ADC, USB interface and USB-based FPGA control and configuration strategy highlighting the end-to-end ADC-to-host PC datapath.

Data processing techniques and preliminary results are discussed. Oscillatory power structures along the meteor electron trail inconsistent with classical Fresnel interval scattering are investigated.

Mesosphere and Lower Thermosphere Lidar Studies

MLTL-01 Design and Development of LabVIEW-Based Novel Software for MRI Lidar System by Zhangjun Wang

Status of First Author: Student NOT in poster competition PhD

Authors: Zhangjun Wang, John A. Smith, Johannes Wiig, Wentao Huang, Xinzhao Chu

Abstract: The lidar technique is an efficient tool for continuous monitoring of global temperature, wind, and aerosol profiling through the middle and upper atmosphere with high accuracy, precision, and resolution. We are developing a Major Research Instrumentation mobile Fe-resonance/Rayleigh/Mie Doppler lidar funded by the National Science Foundation(NSF). This lidar will provide simultaneous measurements of temperature (30-110km), wind (75-110km), Fe density (75-115km) and aerosol (10-100km) in both day and night. A lidar data acquisition and analysis system based on the LabVIEW was developed to collect, process, store, and display data. Here we present the mobile Doppler lidar software system and show the implementation of LabVIEW's virtual interfaces to the modules present at the lidar system. We will give a description of the software system architecture and the retrieval method of temperature, wind, Fe-density and aerosol. The software is able to handle, in real time, MRI lidar signals acquired in photon counting modes and control laser,

telescope and other hardware. Several user-friendly interfaces are available, showing the system parameters, the raw signals, the laser frequency locking condition and all the data products. At last, we will present the data format designed for MRI lidar.

MLTL-02 Robust seed laser frequency stabilization for narrowband Doppler lidars
by John Anthony Smith

Status of First Author: Student IN poster competition PhD

Authors: John Smith, Xinzhao Chu, Wentao Huang

Abstract: Narrowband sodium Doppler lidars require output pulses with a specific center frequency and narrow linewidth to obtain bias-free temperatures and precise wind measurements from the mesosphere, lower thermosphere (MLT). Dye ring lasers are used in many of these systems to seed such properties onto outgoing pulses. Absolute frequency stability is achieved by locking the dye ring laser to a Doppler-free atomic spectral feature of sodium. However, locking precision and stability can be degraded significantly by inadequate performance of the locking system. Taking advantage of the excellent short-term stability of dye ring lasers and the latest in digital technologies, we were able to develop a locking system that achieves an order-of-magnitude improvement in stability across various time scales over previous systems. The flexibility of this locking system enables application to a wide variety of lasers, including piezo-tuned external cavity diode lasers. A function used to detect lost lock conditions with an audible warning proved useful for the potassium Doppler lidar at Arecibo Observatory. We introduce the ‘2-f’ technique; a way to characterize the disturbance introduced by modulating a laser. In addition, we present several other techniques which have assisted us in the design of this robust locking system.

MLTL-03 Recent advances in midlatitude long-term temperature variations deduced from Na lidar observations with brief summary of tidal and mean temperature/wind climatology by Chiao-Yao She

Status of First Author: Non-student

Authors: Chiao-Yao She, David A. Krueger and Tao Yuan, Physics Department, Colorado State University, USA, joeshe@lamar.colostate.edu

Abstract: The Colorado State University (CSU) sodium lidar, first light in August 1989, has conducted regular observations of nocturnal mesopause region temperature and Na density for more than 18 years since May 1991. Between 1993 and 1997, many technological innovations led to improved capabilities, enabling full-diurnal-cycle (24 hour continuous), simultaneous mesopause region temperature and zonal and meridional wind (TUV) observations, weather permitting. Since 2002, the hourly mean Na density, temperature, zonal and meridional wind profiles at 2 km vertical resolution deduced from CSU lidar observations have been deposited in the CEDAR data base for community use. The data from full diurnal cycle observations are most suitable for climatological studies of tidal-period perturbations and tidal-removed mean states in all three dynamical fields. The long-term nocturnal temperature data are of course suited for the evaluation of solar cycle effects and temperature trends.

In this poster, we present recent advances in climatology and long-term study with the emphasis on the latter. The long-term nocturnal temperature record (1990-2007) has been used to reveal episodic response after Mt. Pinatubo eruption, 11-year solar cycle effects and temperature trends. Though the observed cooling reported in the literature from different instruments at different geographic locations is inconclusive, ranging between 0 and 10 K per decade, when all 3 long-term effects are included, the CSU data produced a temperature trend [She et al., JASTP, in press] with maximum cooling of ~ 1.5 K/decade at 91 km and a profile in general agreement with HAMMONIA and SMLTM model predictions. In addition, recently published mean-state and semidiurnal tidal climatology in temperature and zonal and meridional winds by Yuan et al. [JGR, 2008a; 2008b] will be briefly summarized with the emphasis on the comparison with the prediction of leading GCM models (HAMMONIA, TIME-GCM and WACCM3), and on a physical understanding of the observed seasonal variations.

MLTL-04 Rayleigh Lidar Observations of the Arctic Stratosphere and Mesosphere during the International Polar Year - by Brita K Irving

Status of First Author: Student IN poster competition Undergraduate

Authors: Brita K. Irving, Brentha Thurairajah, Richard L. Collins, V. Lynn Harvey

Abstract: Rayleigh lidar density and temperature measurements of the stratosphere and mesosphere (40 – 80km) have been made at Poker Flat Research Range (PFRR), Chatanika, Alaska (65°N, 147°W) during the International Polar Year (IPY), 2007-2008 and 2008-2009. We review the Rayleigh lidar technique and highlight observations during the IPY by presenting the thermal structure of the stratosphere and mesosphere. Stratospheric warming has been recorded in both the 2007-2008 and 2008-2009 winters. Comparisons will be made with previously published monthly mean temperatures from 1997-2005 taken over Chatanika. We will also identify and characterize mesospheric inversion layers (MILs) and discuss the observed temperature structures at PFRR in the context of the synoptic structure of the arctic middle atmosphere.

MLTL-05 Gravity Wave Activity in the Arctic Middle Atmosphere: Rayleigh Lidar Measurements and Analysis - by Brentha Thurairajah

Status of First Author: Student IN poster competition PhD

Authors: Brentha Thurairajah (1), Richard L. Collins (1), V. Lynn Harvey (2)
(1) University of Alaska Fairbanks, Alaska; (2) University of Colorado, Boulder

Abstract: Direct observations of gravity wave activity in the upper stratosphere using high resolution Rayleigh lidar data from Poker Flat Research Range, Chatanika, Alaska (65°N, 147°W) combined with re-analysis data of stratospheric vortex and anticyclones are used to study how these synoptic structures and planetary wave activity modulate gravity wave activity and impact the wintertime middle atmospheric circulation. Gravity wave activity in the 40-50 km altitude region is characterized in terms of wave potential energy density. The gravity wave activity is compared over three meteorologically different winters (2002-2003, 2003-2004, and 2004-2005) and to the structure and evolution of the vortex and anticyclones during these winters. The wave activity is found to be lower during the 2003-2004 winter when a major warming in early January led to the reformation of a vertically displaced stratopause and a two month long disruption of the lower and mid stratospheric vortex. The wave activity is found to be positively correlated to the background flow in the stratosphere. This analysis is extended to include lidar measurements from an Arctic network of lidars as part of the International Polar Year project, Pan-Arctic Studies of the Coupled Tropospheric, Stratospheric, and Mesospheric Circulation [<http://research.iarc.uaf.edu/IPY-CTSM/>]. To avoid bias and maintain consistency the same data processing algorithms have been used to process the data from the various Arctic network of lidars.

MLTL-06 Possible Relations between Meteors, Enhanced Electric Density Layers and Sporadic Sodium Layers - by Xianghui Xue

Status of First Author: Non-student

Authors: Xianghui Xue

Abstract: Using lidar, meteor radar and COSMIC observational data, the Possible Relations between the meteors, the enhanced electric densities and the sporadic sodium layers are found.

MLTL-07 Convective and dynamic stabilities, large wind shears in the mesopause observed by Na lidar at Fort Collins, CO (41°N, 105°W) - by Jia Yue

Status of First Author: Student IN poster competition PhD

Authors: Jia Yue, Chiao-Yao She, Colorado State University; Han-Li Liu, NCAR HAO, Tao Yuan, Colorado State University

Abstract: Between May 2002 and April 2006, over 3000 hours of full-diurnal-cycle observations of mesopause region temperature and horizontal wind have been made by the Colorado State University sodium lidar at Fort Collins, CO (41°N, 105°W). These data have been analyzed in 1 km and 15 min resolution for the characterization of the structure and seasonal variation of Brunt-Vaisala frequency (N) and wind shears. Using these lidar observed high resolution temperature and winds, we address three related science objectives in this poster.

First, we investigate nocturnal atmospheric instabilities in the mesopause region (80-105 km). The probability of convective instability was found to peak in winter at ~ 9% in contrast to the dynamic instability of ~ 10% near equinox. The year-long altitude-averaged N₂, wind shear and Richardson number are found to be $4.29 \times 10^{-4} \text{ s}^{-2}$, 20.1 ms⁻¹km and 0.81, respectively.

Second, we note that the vertical distribution of large wind shears at 80-105 km observed by lidar is similar to those observed by chemical release experiments [Larsen, 2002]. With information on both temperature and winds, we investigate the seasonal dependence of the observed strong correlation between N₂ and large wind shear. The observed correlation is shown to be consistent with the suggestion of Liu [2007], which accounts for the existence of large wind shears above the mesopause.

Third, by removing the tidal perturbations from the data, we present case studies and investigate the effect of large amplitude gravity waves on wind shear and N₂.

MLTL-08 Simultaneous Wind and Temperature Measurements from Lower to Upper Atmosphere by Wentao Huang

Status of First Author: Non-student

Authors: Wentao Huang¹, Xinzhao Chu¹, Johannes Wiig¹, Bo Tan¹, Chihoko Yamashita¹, T. Yuan², J. Yue², S. D. Harrell², C.-Y. She², B. P. Williams³, J. S. Friedman⁴, and R. M. Hardesty⁵

¹University of Colorado at Boulder, 216 UCB, CIRES, Boulder, Colorado 80309

²Colorado State University, Fort Collins, Colorado 80523

³Northwest Research Associates Colorado Research Associates, 3380 Mitchell Lane, Boulder, Colorado 80301

⁴National Astronomy and Ionosphere Center Arecibo Observatory, HC-03 Box 53995, Arecibo, Puerto Rico 00612

⁵National Oceanic and Atmospheric Administration Earth System Research Laboratory, Boulder, Colorado 80305

Abstract: To study the important atmospheric process of wave coupling among different layers, it is crucial to trace waves from their source regions in the lower atmosphere to their dissipation regions in the middle and upper atmosphere. This requires the profiling of wind and temperature simultaneously from the lower to the upper atmosphere. Various types of Doppler lidars can measure wind and/or temperature in different regions; however, none of the single lidar can profile both variables throughout the atmosphere. Resonance fluorescence Na Doppler lidars measure wind and temperature simultaneously in the mesosphere and lower thermosphere. Unfortunately, their measurements are limited to 80-105 km where the trace gas Na atoms are available. We investigated incorporating a Na double-edge magneto-optic filter (Na-DEMOF) into the receiver of a 3-frequency Na Doppler lidar to extend its measurements into the lower atmosphere. Laboratorial experiments were conducted to optimize the filter design and characterize the filter functions, which were also verified by quantum mechanical calculation. Lidar simulations were conducted to assess its performance. We then demonstrated the first simultaneous wind and temperature measurements at Colorado State University. Reliable winds and temperatures were obtained in the altitude range of 10–45 km with 1 km resolution and 60 min integration under the conditions of 0.4 W lidar power and 75 cm telescope aperture. This edge filter with a multi-frequency lidar concept can also be applied to other direct-detection Doppler lidars for profiling both wind and temperature simultaneously.

Mesosphere and Lower Thermosphere Gravity Waves

MLTG-01 High frequency gravity wave observations at UAO - by Chad Carlson

Status of First Author: Student NOT in poster competition PhD

Authors: Chad G. Carlson, Alan Liu, Gary R. Swenson

Abstract: In this work, we report on high frequency atmospheric gravity wave signatures (< 30 min) in sodium lidar temperature and density data taken at the Urbana Atmospheric Observatory. Several nights of observations from 2007-2009 will be presented and the methodology of extracting the high frequency data will be discussed.

MLTG-02 Gravity wave effects on polar mesospheric clouds: A comparison of numerical simulations with AIM observations - by Amal Chandran

Status of First Author: Student IN poster competition PhD

Authors: A. Chandran^{1, 2,*}, D. W. Rusch¹, A. W. Merkle¹, S. E. Palo², G. E. Thomas¹, E. J. Jensen⁴, M. J. Taylor³

¹ Laboratory for Atmospheric and Space Physics, University of Colorado, Boulder

² Department of Aerospace Engineering, University of Colorado, Boulder

³ Center for Atmospheric and Space Sciences and Physics Department, Utah State University, Logan, UT

⁴ NASA AMES center, San Francisco

Abstract: In this presentation we present preliminary results from the Community Aerosol and Radiation Model for Atmospheres (CARMA 2D) model of the effects of atmospheric gravity waves (AGW) on Polar Mesospheric Clouds (PMC). The model shows differences in ice particle size and brightness of PMCs depending on the scale and periods of the AGWs. We present comparisons between our numerical simulations and observations from the Cloud Imaging and Particle Size (CIPS) experiment on board the Aeronomy of Ice in the Mesosphere (AIM) spacecraft. CIPS images have shown distinct wave patterns and structure in Polar Mesospheric Clouds (PMCs), around the summertime mesopause region, which are qualitatively similar to ground based photographs of Noctilucent Clouds (NLCs). The structures observed in PMCs have generally been considered to be manifestations of upward propagating AGWs. CIPS results show a distinct anti-correlation of wave structures detected in PMCs with PMC occurrence frequency and strong correlations with temperature perturbations supporting the idea of gravity wave induced cloud sublimation. Maps of the locations of the observed wave events in the PMC fields show regions of high wave activity in both hemispheres. The propagation directions of the waves are considered to infer information about possible sources for the AGWs at polar latitudes.

MLTG-03 Mesospheric Atmospheric Gravity Waves Observed by Rayleigh-Scatter Lidar by Durga Nath Kafle

Status of First Author: Student IN poster competition PhD

Authors: Durga N Kafle and Vincent B Wickwar

Abstract: Approximately 900 nights of observations with a Rayleigh-scatter lidar at Utah State University's Atmospheric Lidar Observatory (41.7°N, 111.8°W), spanning the 11-year period from late 1993 through 2004, have been reduced to derive nighttime temperature and relative density profiles between 45 and 90 km, i.e., over the entire mesosphere. Of these, 150 profiles that extend to 90 km or above were used in this work, which is based mainly on relative density data with 3-km altitude resolution and 1-hour temporal resolution. This is, we believe, the first comprehensive study of monochromatic gravity waves using Rayleigh-scatter lidar observations extending through the entire mesosphere at mid-latitudes. The variations of relative density perturbations were used to identify the presence of monochromatic gravity waves. These waves have a clear downward phase progression (i.e. upward energy propagation) with the most prevalent vertical phase velocity (c_z) of 0.6 ms⁻¹ (2.2 km/hr). The most dominant vertical wavelength (λ_z) is 12 km. The values of the Brunt-Väisälä frequency, (N , rad/sec), the maximum gravity wave frequency, were calculated by using seasonally averaged nightly temperature and temperature derivative profiles. Using the gravity wave dispersion relations and the values of c_z , λ_z , and N , other gravity wave parameters such as wave period (T), horizontal wavelength (λ_h), horizontal phase velocity (c_h), and horizontal distance to the source region (R) were calculated. The most prevalent values of T , λ_h , and R are 6 hours, 550 km, and 35 ms⁻¹ (125 km/hr), respectively. The most dominant values of λ_h for 45-km and 90-km altitudes are 2500 km and 5000 km, respectively, which suggest that these large-scale gravity waves are generated from a very distant and very extended source region. There appears to be a seasonal dependence in T , λ_h , and R but not in c_z and λ_z . The vertical phase velocities maximized in summer whereas the apparent periods, horizontal wavelengths, and horizontal distance to the source region maximized in winter. The magnitude of the relative density perturbations on average grew with altitude with an e -folding distance of 20 km, which is larger than the H km expected for undisturbed gravity wave propagation, where H is the scale height. This means

that the amplitude of the observed fluctuations increases less rapidly with altitude than for the undisturbed situation, which also implies that significant gravity-wave energy dissipation occurs in this region.

MLTG-04 Seasonal and inter-annual variability of gravity wave activity revealed from long-term lidar observations over Mauna Loa Observatory, Hawaii - by Tao Li

Status of First Author: Non-student

Authors: Tao Li, School of Earth and Space Sciences, University of Science and Technology of China, Hefei, Anhui, China
Mengcheng National Geophysical Observatory, Mengcheng, Anhui, China
Thierry Leblanc, I. Stuart McDermid, Table Mountain Facility, Jet propulsion Laboratory, California Institute of Technology, Wrightwood, California, USA
Dong L. Wu, Jet propulsion Laboratory, California Institute of Technology, Pasadena, California, USA
Xiankang Dou, and Shui Wang, School of Earth and Space Sciences, University of Science and Technology of China, Hefei, Anhui, China

Abstract: With the 10.5 years-long (January 1997 to June 2007) temperature data obtained by the Jet Propulsion Laboratory (JPL) Rayleigh lidar at Mauna Loa Observatory (MLO), Hawaii, the seasonal and inter-annual variability of gravity wave (GW) variances was revealed in the upper stratosphere (35-50 km) and lower mesosphere (48-63 km) respectively. The estimation of wave energy suggests that the potential energy was significantly lost when the GWs propagated upward across the stratopause. In the upper stratosphere, the winter maximum and summer minimum were observed, suggesting the dominance of annual oscillation (AO). While in the lower mesosphere, the seasonal oscillations of GW variances for the waves in the long vertical wavelength band (4-15 km) were dominated by semiannual oscillation (SAO), likely due to the selectively filtering of GWs by the tropical stratospheric SAO wind. The QBO modulation was clearly present only in the upper stratosphere for the long vertical wavelength band, but not in the lower mesosphere. The United Kingdom Meteorology Office (UKMO) zonal mean zonal wind further suggested that the enhanced GW activities corresponded to the easterly shear phase of QBO wind and the suppressed activities corresponded to the westerly shear phase. During the strong El Niño event in the winter 1997/1998, the enhanced GW activities were observed only for the long vertical wavelength band in the lower mesosphere, but not in the upper stratosphere, consistent with the early model prediction and observed temperature response in the mesosphere of subtropical region. The additional enhancement of GW variances was also found during the solar maximum during 2001-2002 and prior to 2006 major Sudden Stratospheric Warming (SSW).

MLTG-05 Intra-Annual Comparison of Mesospheric Gravity Waves Over Halley and Rothera Stations, Antarctica - by Jonathan Rich Pugmire

Status of First Author: Student IN poster competition Undergraduate

Authors: J.R. Pugmire, M.J. Taylor, K. Nielsen, A. Wall, J. Thompson, P.D. Pautet; Center for Atmospheric and Space Science and Physics Department, Utah State University, Logan, UT, U.S.A.

Abstract: As part of a collaborative program between British Antarctic Survey and Utah State University, we present an intra-annual study of short-period, mesospheric gravity wave events observed over Antarctica in the near infrared OH emission. The measurements were made using an all-sky airglow imager operated at either Halley Station (76° S, 27° W) on the Brunt Ice Shelf, or Rothera Station (68°S, 68°W), situated on the Antarctic Peninsula. A total of six austral winter seasons have been analyzed (2000-2006). This study comprises the first detailed winter seasonal investigation of short-period mesospheric gravity waves at high-Antarctic latitudes. Distributions of their observed wave parameters were found to be similar to previous findings using imaging instrumentation at other latitudes in the Northern and Southern Hemispheres. However, the observed wave headings exhibited strong, but dissimilar anisotropy at both sites that was also found to be repetitive from year to year, establishing a persistent recurrent pattern. In this poster we present example wave data and seasonal summaries of their properties at both observing sites focusing on wave anisotropy and the strong year to year consistency.

MLTG-06 Ripple Climatology Observed in the Mesopause Region over Maui, Hawaii

by Deepak B. Simkhada

Status of First Author: Student IN poster competition PhD

Authors: Deepak B. Simkhada, d.simkhada@aggiemail.usu.edu; Michael J. Taylor, mike.taylor@usu.edu, Utah State University, Center for Atmospheric and Space Sciences, Physics Department

Abstract: Airglow imaging observations have been analyzed to investigate small-scale wave-like patterns, known as ripples, and their horizontal characteristics in the mesopause region over Maui, Hawaii (20.70 N, 156.30 W). Measurements were obtained by using the Utah State University (USU) Mesospheric Temperature Mapper (MTM), a high performance imaging system, based on the OH and O₂ nightglow emission layers centered at altitudes of ~87 km and ~94 km, respectively. A total of the 360 events in OH emission and 347 events in O₂ emission (219 coincident events) were recorded during 2003-2004 periods, exhibiting horizontal wavelengths of ~6-16 km, phase speeds of ~20-50 m/s, observed periods of ~5-10 min and lifetimes of ~16-48 min. Seasonal investigation of the ripples occurrence frequency, horizontal wavelengths and phase speeds showed no preference. However, the horizontal propagation directions showed clear azimuthal anisotropy. In this poster, we focus on the climatology and statistical studies of small-scale ripples in the low latitude mesopause region and compare their properties with large-scale gravity wave events.

MLTG-07 Mesospheric Gravity Waves Over Equatorial Brazil - by Camille Briana Smith

Status of First Author: Student IN poster competition Undergraduate

Authors: Camille B. Smith, M.J. Taylor, P.-D. Pautet, A. Fragoso, H. Takahashi

Abstract: As part of a collaborative investigation of mesospheric dynamics with Instituto Nacional de Pesquisas Espaciais (INPE), Brazil, we made two-station all-sky image measurements over equatorial Brazil from November 2005 to April 2007. Examining the airglow data, we observed a variety of gravity wave activity in the mesospheric OH emissions (peak height 87 km), including gravity wave bands, ripple instabilities, and Bore events over Monteiro, Brazil (7.9° S, 37.1° W). Here we report detailed analysis of these events and their frequency of occurrence during different times of the year.

MLTG-08 Tri-station Observation of Polar Mesospheric 10-hr Inertio Gravity Wave

by Qian Wu

Status of First Author: Non-student

Authors: Qian Wu^{1,5}, S. Nozawa², C. Hall³, C. Meek⁴, A. Manson⁴, Jiyao Xu⁵, J. M. Russell III⁶

1. High Altitude Observatory, National Center for Atmospheric Research, P.O. Box 3000, Boulder, Co 80307-3000

2. STEL, Nagoya University, Chikusa-ku, Nagoya, 464-01, Japan.

3. Faculty of Science, University of Tromsø, Tromsø, Norway.

4. Institute of Space and Atmospheric Studies, University of Saskatchewan, Saskatoon, Saskatchewan, Canada.

5. State Key Laboratory of Space Weather, Center for Space Science and Applied research, Chinese Academy of Sciences, Beijing, China.

6. Hampton University, Hampton, Virginia

Abstract: Using mesospheric and lower thermospheric wind measurements from Resolute (75N), Eureka (80N), and Bear Island (74N), we examine a 10-hr inertio gravity wave (IGW) event at very high latitudes. This is probably the first time a short vertical wavelength (~20 km) IGW is observed at the high latitude with multi-stations. With satellite data based buoyancy frequency and dispersion equation, the horizontal wavelength of the wave was estimated to be about ~2500 km. That horizontal wavelength is consistent with inter-station phase difference. The wave was propagating mostly in the meridional direction, which may imply the wave source is at lower latitudes. The IGW has a very large horizontal scale as seen by three stations. The wave peaks around 90 km altitude, no significant amplitude above 100 km was observed which is not consistent with some model simulation predictions. IGW is a major dynamic feature in the polar mesosphere, a better characterization of the wave will go a long way towards a better understanding of various forcings that affecting the region.

MLTG-09 Investigations of wave-induced secular variations of exothermic heating in the MLT region -
by Robert Thacker-Dey

Status of First Author: Student IN poster competition Undergraduate

Authors: Robert Thacker-Dey, Penn State, email: rpt5017@psu.edu, (O) 215-760-7187
Tai-Yin Huang, Penn State Lehigh Valley, email: tuh4@psu.edu, (O)610-285-5100
Michael Hickey, Embry-Riddle Aeronautical University, email: Michael.hickey@erau.edu, (O) 386-226-7059

Abstract: This study aims to examine wave-induced secular variations of exothermic heating in the MLT region with a 2D OH chemistry-dynamics model that simulates the wave-induced response of the minor species. A wave packet that provides wave forcing is simulated with a spectral full wave model. Total cumulative exothermic heating reveals the greatest fluctuation to occur at 320 minutes after the time simulation, increasing around 95 km altitude where downward transport of minor species occurs below this altitude. The maximum increase of exothermic heating rates occurs just below 90 km at the end of the simulation (~520 min), consistent with expected high level densities of odd-hydrogen and oxygen constituents. Each chemical reaction involved in the OH nightglow chemistry is to be considered and analyzed along with its contribution of exothermic heating in the MLT region.

MLTG-10 Case Study of an Inertia-Gravity Wave in the Mesosphere over Alaska with the Poker Flat Incoherent Scatter Radar - by Roger Hale Varney

Status of First Author: Student IN poster competition PhD

Authors: R. H. Varney, M. J. Nicolls, S. L. Vadas, P. Stamus, C. J. Heinselman, and M. C. Kelley

Abstract: A case study of mesospheric winds and waves observed by the Poker Flat Incoherent Scatter Radar (PFISR) on April 23, 2008 is presented. Active aurora created sufficient ionization for nearly 12 hours of continuous incoherent scatter measurements from the D-region ionosphere from ~60-90 km. PFISR utilized a multi-look-direction mode which permitted measurements of vector winds, in addition to high precision vertical velocity measurements, at high temporal resolution. A large-amplitude wave with a downward phase velocity and a long period, over 8 hours, was observed. The proximity of this period to the local inertial period in addition to its large horizontal wavelength suggest that this wave is an inertia gravity wave (IGW). The hodographs display the characteristic elliptical polarization of IGWs and fits of the hodographs allow for estimation of the Earth-frame periods. Vertical wavelengths are measured directly and found to be in the range of 4-10 km, increasing with altitude, strongly implying propagation against the background winds. Mean background winds are found to increase to the west with altitude, with some small meridional components developing at later times. Linear theory is used to derive horizontal wavelengths and the direction of propagation, which confirm propagation against the winds.

MLTG-11 A Spectral Parameterization of Drag, Heating and Eddy Diffusion for a Three-Dimensional Mean Flow Induced by Breaking Gravity Waves - by Xun Zhu

Status of First Author: Non-student

Authors: Xun Zhu, Jeng-Hwa Yee, William Swartz, Elsayed Talaat

Abstract: There are three distinct processes by which upward propagating gravity waves influence the large-scale dynamics and energetics in the mesosphere and lower thermosphere: (i) non-localized transport through wave propagation that remotely redistributes the atmospheric momentum from the wave generation to dissipation regions, (ii) localized transport by perturbing wave structures that redistributes the thermal energy within a finite domain, and (iii) localized diffusive transport of both momentum and heat due to mixing induced by wave dissipation. These effects become most significant for breaking waves when momentum drag, dynamical heating and eddy diffusivity are all imposed on a background state. A three-dimensional spectral parameterization algorithm has been developed to simulate all these processes in a general circulation model or to diagnose them in a measured large-scale wind field. For a given input wind profile (u,v) as a basic state at a model grid, the parameterization algorithm outputs the vertical profiles of drag, heating and eddy diffusion coefficients that allow one to calculate all the force terms on the right sides of the momentum and energy

equations. It is found that the in situ dynamical cooling/heating near the summer/winter mesopause by the gravity wave breaking could be important in determining both the local temperature and the meridional circulation. Additional results of applying the algorithm to the JHU/APL two-dimensional model and the TIMED/SABER derived winds will also be presented.

MLTG-12 Observation and modeling of OH airglow temperature and intensity perturbations by mesospheric gravity waves – Jonathan Snively

Status of First Author: Non-student

Authors: Jonathan Snively (jonathan.snively@usu.edu), Michael Taylor (mike.taylor@usu.edu), Dominique Pautet (dominiquepautet@gmail.com), Deepak Simkhada (d.simkhada@aggiemail.usu.edu)

Atmospheric gravity waves at a broad range of temporal and spatial scales are frequently observed in MLT airglow imaging experiments. Airglow data provide significant insight into gravity wave propagation, directionality, and seasonality, and allow estimations of wave fluxes [e.g., Swenson et al., JGR, 104(D6), 1999]. The USU / CEDAR Mesospheric Temperature Mapper (MTM) is a specialized CCD airglow imaging system, which was operated at Maui MALT from November 2001 to December 2006. It captures OH(6,2) and O₂(0,1) emissions intensities, filtered to allow determination of airglow rotational temperature [Meriwether, MAP Handb., 13, 1984]. The MTM has been used previously to assess zenith temperatures, showing close agreement with lidar temperature data [Zhao et al., J. Geophys. Res., 110, D09S07, 2005], in addition to two-dimensional structure of intensity and temperature perturbations associated with small-scale gravity waves [Taylor et al., Rev. Bras. Geof., 25, 2007].

Here we investigate the horizontal structure of relatively small-scale gravity wave perturbations captured by the MTM, as both intensity and rotational temperature. Using a photochemical-dynamical model for the OH(6,2) emission, coupled with a two-dimensional numerical model for gravity wave dynamics [Snively and Pasko, JGR, 113, A06303, 2008], we construct case studies to allow direct comparisons with observed data. The Krassovsky ratios and integrated cancellation effects [e.g., Swenson and Gardner, 103(D6), 1998] of the modeled and observed airglow signatures are investigated and compared. Limitations of the model and data are discussed, along with implications for gravity wave momentum flux calculations.

MLTG-13 Mesospheric Front in a Doppler Duct Observed over Ferraz Station, Antarctica (62°S) - by José Valentin Bageston – presented by Igo Paulino

Status of First Author: Student NOT in poster competition PhD

Authors: J.V. Bageston, C.M. Wrasse, D. Gobbi, H. Takahashi, I. Paulino, R. E. Hibbins, D. C. Fritts

Abstract: On 16-17 July, 2007 during an observational campaign at Ferraz Station, Antarctica (62°S, 58°W), a mesospheric front was observed with an airglow all-sky imager. The event appeared like an extensive dark front on OH airglow emission. Simultaneous mesospheric winds measured with MF radar at Rothera Station, Antarctica (67°S, 68°W) and temperature profiles from SABER instrument, on board of TIMED satellite, were used to obtain the propagation condition for this wave. Also, the physical properties of the front are calculated by applying the standard FFT analysis. A collocated imaging spectrometer, OH(6-2), for mesospheric temperature measurements, has been operated simultaneously with the all-sky imager. Direct effects of the mesospheric front have been seen in imaging spectrometer measurements, showing an abrupt decrease in both OH intensity and rotational temperature when the front passes overhead.

MLTG-14 Estimation of large scale gravity wave parameters using airglow images by Igo Paulino

Status of First Author: Student NOT in poster competition PhD

Authors: I. Paulino [1], H. Takahashi [1], C. M. Wrasse [2], D. Gobbi [1], A. F. Medeiros [3] and R. A. Buriti [3] [1] Instituto Nacional de Pesquisas Espaciais, SP/Brazil, [2]Universidade do Vale do Paraíba, SP/Brazil, [3]Universidade Federal de Campina Grande, PB/Brazil.

Abstract: From the mesospheric airglow all sky image observation, gravity wave characteristics (wavelength, phase velocity, period, propagation direction) has been calculated by using Fourier transform spectral analysis. However determination of the wavelength, for example, is limited due to limited sky view. There is a difficulty to determine the horizontal wavelength longer than 100-150 km by this technique. A new technique to estimate long wavelength gravity waves is required. It is presented, in this work, an algorithm to calculate the large scale mesospheric gravity wave parameters from a sequence of all sky airglow images. As a first step, Keogram was constructed by extracting north-south and east-west slices of unwarped airglow images and building a new image in a temporal sequence. In the new image Fourier analysis was applied, in order to calculate the period. With the period it is possible to estimate the phase velocity for each component. Then, the wavelength and the phase propagation direction will be calculated. Some results by this technique will also be presented.

Mesosphere and Lower Thermosphere Other Tidal or Planetary Waves

MLTT-01 Influence of an Ultra Fast Kelvin Wave on the Migrating Diurnal Tide by Loren Chang

Status of First Author: Student IN poster competition PhD

Authors: Loren Chang, Department of Aerospace Engineering Sciences, University of Colorado
Scott Palo, Department of Aerospace Engineering Sciences, University of Colorado
Han-Li Liu, High Altitude Observatory, National Center for Atmospheric Research

Abstract: The migrating diurnal tide is one of the dominant dynamical features of the Earth's Mesosphere and Lower Thermosphere (MLT) region, particularly at low latitudes. While the long term evolution of the migrating diurnal tide is dependent primarily upon seasonal changes in the solar heating profile and the background atmosphere, short term fluctuations on the order of a few days have been observed, occurring at time scales too short to be explained by changes in solar heating. However, the mechanisms, underlying physical processes, and overall effects of a planetary wave / tidal interaction are still unclear.

In this study, we explore the affect of an ultra fast Kelvin waves (UFKWs) on the migrating diurnal tide using the NCAR Thermosphere Ionosphere Mesosphere Electrodynamics General Circulation Model (TIME-GCM). The UFKWs are eastward propagating disturbances that occur sporadically throughout the year in the low latitude MLT region where the migrating diurnal tide is large. The results of the numerical experiments have indicated the UFKW modulates the global amplitude of the dominant diurnal [1,1] tidal mode at the period of the UFKW, while causing a shift in the tidal horizontal wind structure towards the Equator. Scale analysis of the background atmosphere and tidal tendencies is also performed to identify the mechanisms responsible for the aforementioned changes.

MLTT-02 Longitude Variations of the Solar Semidiurnal Tides in the Mesosphere and Lower Thermosphere at Low Latitudes Observed from Ground and Space - by Jonathan S Friedman

Status of First Author: Non-student

Authors: Friedman, J. S., Zhang, X., Chu, C., Forbes, J. M.

Abstract: We present an analysis of longitudinal variation in the solar semidiurnal tide observed in the nocturnal thermal structure of the low-latitude mesopause region (83–103 km) at low latitudes. Ground-based lidar measurements from two sites, Arecibo, Puerto Rico and Maui, Hawaii are coupled with space-based observations by the SABER instrument aboard the TIMED satellite. Results are compared with the GSWM-02 model.

MLTT-03 The Seasonal and Intraseasonal Variation of the Diurnal Tide in the Mesosphere and Lower Thermosphere Observed by Meteor Radar over Maui, HI (20.7o N, 156.3o W) - by Xian Lu

Status of First Author: Student IN poster competition PhD

Authors: Xian Lu (xianlu2@illinois.edu), Alan Z Liu (liuzr@illinois.edu), Steven Franke (s-franke@illinois.edu)

Abstract: Wind measurements by the meteor radar from the year 2002 to 2007 were used to study the seasonal and intraseasonal variations of the diurnal tide in the mesosphere and lower thermosphere (MLT) over Maui, HI (20.7° N, 156.3° W). The amplitudes of the diurnal tide were found to be larger at equinoxes and smaller at solstices. The amplitudes are largest at 93~94 km in spring, which is different from GSWM00 simulation that has the strongest diurnal tide in October at ~103 km at the same latitude.

The phases of the diurnal tide show downward progression thus upward energy propagation. A quasi-annual cycle persists in tidal phases and on average, there is a 5- to 7-h phase shift between winter and summer.

It was found that diurnal tides propagate upward without much dissipation and reach the maximum amplitudes between 90 and 97 km, above which severe dissipation occurs and the amplitudes decrease dramatically with the altitude.

Lomb-Scargle periodogram was applied to evaluate the seasonal and intraseasonal variations of the tidal amplitudes. For both zonal and meridional wind components, the annual cycle variation dominates below 88 km and semiannual cycle dominates above it. Besides the dominant annual and semiannual cycles, intraseasonal variations are also very significant, among which the 4-month, 3-month and 70~80-day oscillations are especially strong in modulating the tidal amplitudes. Variations of gravity wave activity were also evaluated and correlated with the tidal variability to examine their relationships.

MLTT-04 A Collaborative Study on Temperature Diurnal Tide in the midlatitude Mesopause region by Na lidar (41°N, 105°W) and TIMED/SABER - by Tao Yuan

Status of First Author: Non-student

Authors: Tao Yuan

Abstract: The Na lidar at Colorado State University (41°N, 105°W) has observed mesopause region temperature, zonal and meridional winds over full diurnal cycles, for nearly five thousand hours from May 2002 to December 2008. Harmonic analysis on this unique data set yields a monthly climatology of diurnal tidal period perturbations of temperature and winds. In this poster, the observed temperature diurnal tidal perturbations are compared with tidal measurements by the TIMED/SABER instrument for the first time to elucidate the global context of temperature diurnal tidal perturbations observed locally by the ground based lidar. With this comparison, we identify the migrating tide as the dominant tidal component within the mesopause region above Fort Collins, thus determining most of the seasonal variations of diurnal modulation. Although the satellite observations exhibit some similar tidal seasonal variations, the lidar measured diurnal amplitudes during the winter months are considerably larger than the SABER tidal observations, so that a single diurnal amplitude minimum in summer solstice is found in lidar observed seasonal variations, instead of dual amplitude minima during solstice conditions detected by SABER. The lidar-observed large diurnal amplitude in the winter months is accompanied with “trapped” wave behavior with very long vertical wavelength, while the satellite observations show propagating behavior with much shorter vertical wavelength. A detailed study showed that the “anomalous” diurnal perturbation has large day-to-day variations and irregularities, possibly related to local events that are difficult to capture with SABER’s sampling scheme.

MLTT-05 Investigation of Thermospheric Density Modeling on a Diurnal Time Scale by Jung Soo Kim

Status of First Author: Student IN poster competition PhD

Authors: Jung Soo Kim (PSU, Aerospace Engineering, juk211@psu.edu), Julio Urbina (PSU, Electrical Engineering, JUrbina@engr.psu.edu), Timothy J. Kane (PSU, Electrical Engineering and Meteorology, tjk7@psu.edu), David B. Spencer (PSU, Aerospace Engineering, dbs9@engr.psu.edu)

Abstract: In order to estimate thermospheric neutral densities, two empirical thermospheric neutral density models have been widely used; the Jacchia-class model based primarily on drag data obtained from numerous satellites, which is a more operational model, and the MSIS-class (Mass Spectrometer and Incoherent Scatter Radar) model based primarily on the incoherent scatter radar data, which is widely used in the research community. These models have their own strengths and

weaknesses with their data sets. Therefore, we suggest a Blending Technique method in the altitude range of 140 km ~ 200 km using more valid region of each model to compromise each model's weakness. The results show that along-track differences from the Blending Technique are approximately 12 km behind the Jacchia-Bowman's JB2006 model and approximately 4 km ahead the Naval Research Laboratory's NRLMSISE-00 model after 5-day simulation in 2003. The NCAR's physics-based model (TIE-GCM) is compared to the in situ measurements from the CHAMP (CHALLENGING Mini-satellite Payload) satellite and the NRLMSISE-00 model during the geomagnetic storm time on November, 2003. Also, the empirical thermospheric neutral density models (JB2006, JB2008, and NRLMSISE-00) are compared to in situ measurements from the CHAMP satellite during geomagnetic quiet and storm time in 2003. The comparison tells us that the density models need to be developed to estimate neutral densities more precisely on the diurnal time scale. Beginning from the Blending Technique, we will work with the TIE-GCM, optimize it for high temporal rate runs, and begin comparisons with in situ satellite based measurements of the neutral density. Ground-based measurements will be utilized as well, both for comparisons as well as model inputs.

MLTT-06 Observations of 6- and 8- hour period waves at the South Pole - by Pruthvish Bena Patel

Status of First Author: Student IN poster competition Undergraduate

Authors: Pruthvish Bena Patel

Abstract: OH temperature in the mesosphere have been tracked at South Pole Station, Antarctica (90o S) using a Michelson Interferometer. The location provides OH temperature and airglow emission data throughout the six-month winter period. This paper will discuss the observations and modeling of the 6-hour and 8-hour period waves observed in OH rotational temperature data. Mutli-year data collected at the South Pole will be used in the paper to investigate the 6-hour and 8- hour period waves and their monthly characteristics.

MLTT-07 Local Spectral Analysis of very long Radar Wind Time Series - by Bob Stockwell

Status of First Author: Non-student

Authors: R.G. Stockwell, NWRA/CoRA, stockwell@co-ra.com

Abstract: An efficient sampling algorithm for the S-Transform has been developed that greatly reduces the storage requirements of the resulting local spectrum, yet fully represents the entire time-frequency. This addresses the main practical limitation on ST analysis, and allows one to apply the ST to very long time series. Here, hourly measurements of the horizontal MLT winds measured at Hawaii, USA over a 16 year time span are analyzed, showing the temporal variation of the semidiurnal and diurnal tides, two day waves, 15 day planetary waves, and semiannual, annual, and interannual signals.

MLTT-08 Principal Harmonic Analysis of tidal signals in radar winds - by Bob Stockwell

Status of First Author: Non-student

Authors: R.G. Stockwell, NWRA/CoRA, stockwell@co-ra.com

Abstract: High resolution tidal signals are retrieved from radar winds via a novel analysis called Principal Harmonic Analysis. This data adaptive method extracts time-varying quasimonochromatic signals from the data and has the ability to resolve very rapid tidal enhancements such as a diurnal tidal amplitude of 10m/s observed on Feb. 27, 2008, and 6 days later reaching an amplitude of nearly 70 m/s.

Mesosphere or Lower Thermosphere General Studies

MLTS-01 Quiet-Nighttime TIMED/SABER NO+(v) VER Data Characterization at E-region Altitudes - by Jose R Fernandez

Status of First Author: Non-student

Authors: J.R. Fernandez, C. J. Mertens, D. Bilitza, X. Xu, J. M. Russell III, and M. G. Mlynczak

Abstract: The NO+(v) Volume Emission Rate (VER) is a new data product derived from TIMED/SABER limb radiance observations at 4.3 μm . NO+(v) VER can be used as a proxy to study the nighttime E-region during storm-time events by using the so-called Storm-to-Quiet Ratio (SQR). SQR is defined as the ratio of magnetic storm-enhanced NO+(v) VER to a climatological quiet-time NO+(v) VER. This ratio is intended to be used as a magnetic storm-time E-region correction factor to the International Reference Ionosphere (IRI) model electron densities. SABER measurements have been taken continuously since 2002. In this study, quiescent nighttime NO+(v) VER are characterized by grouping scans according to SABER yaw periods during years 2002-2006. Using statistical analysis, the median quiet-time NO+(v) VER profiles and error estimates are determined for each yaw period. The statistical analysis allow us to determine the optimal SQR altitude range to use for the IRI storm-time E-region electron density correction factor.

MLTS-02 Simultaneous OII 7320 Å Line Width and Incoherent Scatter Radar O+ Temperatures Measured at Arecibo - by Pedrina Terra Santos

Status of First Author: Non-student

Authors: Pedrina Terra¹, John Noto², Michael Migliozi², Juannita Riccobono², C.G. M. Brum¹, Raul Garcia¹, Eva Robles¹ and Robert Kerr¹

¹ National Astronomy and Ionosphere Center, Arecibo Observatory, HC-03 Box 53995, Arecibo, PR 00612

² Scientific Solutions Inc., 55 Middlesex Street, North Chelmsford, MA 01863

Abstract: OII 7320 Å line width data were acquired at Arecibo Observatory during the evening and morning twilights since April 2008 using a low resolution single etalon Fabry-Perot Interferometer (FPI). The Arecibo FPI was configured using a 0.9cm spacing plate, producing a free spectral range of 0.298 Å and a spectral resolution of 0.03 Å, sufficient to sample line width temperatures as low as 500K. A very narrow, 3 Å FWHM three-cavity interference filter was used to preclude OH contamination from the 7316.3 Å or 7329.9 Å. In this work three coincident nights of OII 7320 Å line width and Incoherent Scatter Radar (ISR) O+ temperatures are compared and analyzed.

MLTS-03 Development of efficient finite-difference time-domain models of infrasound propagation in a realistic atmosphere - by Sebastien de Larquier

Status of First Author: Student IN poster competition Masters

Authors: Authors: Sebastien de Larquier and Victor P. Pasko

Sebastien de Larquier, CSSL, The Pennsylvania State University, University Park, Pennsylvania 16802, USA

(sdelarquier@psu.edu);

Victor P. Pasko, CSSL, The Pennsylvania State University, University Park, Pennsylvania 16802, USA (pasko@psu.edu);

Abstract: Atmospheric infrasonic waves are acoustic waves with frequencies ranging from 0.02 to 10 Hz, slightly higher than the acoustic cut-off frequency (~ 0.032 Hz), but lower than the audible frequencies (typically 20 Hz-15 kHz) [e.g., Blanc, Ann. Geophys., 3, 673, 1985]. A number of natural events have been identified as generating atmospheric infrasound, such as volcanoes, tornadoes, avalanches, earthquakes [e.g., Bedard and Georges, Physics Today, S3, 32, 2000], ocean surfaces [e.g., Gossard and Hooke, Waves in the Atmosphere, Elsevier, 1975, Ch.9], lightning [e.g., Assink et al., GRL, 35, L15802, 2008; Pasko, JGR, 114, D08205, 2009], and more recently transient luminous events in the middle atmosphere termed sprites [e.g., Farges, Lightning: Principles, Instruments and Applications, H.D. Betz et al., Springer, 2009, Ch.18]. The importance of infrasound studies has also been emphasized in the past ten years from the Comprehensive Nuclear-Test-Ban Treaty verification perspective [e.g., Le Pichon et al., JGR, 114, D08112, 2009]. A proper understanding

of infrasound propagation in the atmosphere is required for identification and classification of different infrasonic waves and their sources [e.g., Drob et al., JGR, 108, D21, 4680, 2003].

We will provide a status report on the development of a finite-difference time-domain (FDTD) model of infrasound propagation in a realistic atmosphere, currently ongoing at Penn State. We use the absorption model of infrasound introduced by Sutherland and Bass [J. Acoust. Soc. Am., 115 (10/2), 2004]. Classical absorption mechanisms as well as molecular relaxation mechanisms are taken into account. The altitude and frequency dependant attenuation coefficients provided by Sutherland and Bass [2004] are included in classical equations of acoustics in a gravitationally stratified atmosphere using a decomposition technique recently proposed by Groot-Hedlin [J. Acoust. Soc. Am., 123 (3), 2008]. We will present representative FDTD results on propagation of infrasonic waves from well-known sources (i.e., aurora).

MLTS-04 Meteoric smoke particle properties derived using dual-beam Arecibo UHF observations of D-region spectra during different seasons - by Jonathan Fentzke

Status of First Author: Student IN poster competition PhD

Authors: Jonathan T. Fentzke (1,2), Diego Janches (1), Irina Strelnikova (3), Markus Rapp (3)

(1) NorthWest Research Associates, CoRA Division

(2) University Colorado at Boulder, Aerospace Engineering Sciences Department

(3) Leibniz Institute of Atmospheric Physics\

Abstract: In this work we present a seasonal study of the presence and characteristics of meteoric smoke particles (MSPs) in the D-region plasma derived from observations using the 430 MHz dual-beam Arecibo Observatory (AO) incoherent scatter radar (ISR) in Puerto Rico (18°N, 67°W). MSPs are believed to be the major source of condensation nuclei for the formation of ice particles, the precursor for a number of MLT phenomena. Our results are obtained by utilizing a method similar to one developed by Strelnikova et al. [2007, Meteor smoke particle properties derived from Arecibo incoherent scatter radar observations, GRL (35)15] who fitted a summed Lorentzian function to the ISR power spectra in order to derive the MSP sizes and number densities. This method allows us to determine mean particle radii and densities in the 80 – 95 km altitude range during the hours of 10 - 14 AO LT when the detected signal-to-noise (SNR) from the D-region is strongest. Our results provide insight into the presence and distribution of meteoric dust in the mesosphere resulting from the condensation of ablated meteoric material. Furthermore, we investigate the existence of any correlation between the seasonal variations of the derived MSPs properties with that of the meteoric input function (MIF) in the MLT above Arecibo.

MLTS-05 An investigation of the impacts of temperature and large-scale circulation on OH airglow using SABER data - by Zhenhua Li

Status of First Author: Student IN poster competition PhD

Authors: Zhenhua Li, Department of Atmospheric Sciences; Alan Z. Liu, Department of Electrical and Computer Engineering, UIUC

Abstract: Using SABER nighttime observation of OH airglow emission rate, temperature, and density from 2003 to 2008, the seasonal variations of airglow intensity, centroid height, and peak volume emission rate in the altitudes of ~70-100 km are examined. Both temperature and descending of O(1S) rich air into the mesopause region play important roles in affecting the volume emission rate of OH layer. Through a simple model, the relationship between OH airglow emission rate, air temperature, and large-scale circulation is investigated.

MLTS-06 Rocket Observations of Lower Thermospheric Winds at High Latitudes During Active Conditions - by Tyler David Scott

Status of First Author: Student IN poster competition Masters

Authors: T. D. Scott (1), M. F. Larsen (1), and J. D. Craven (2), 1Department of Physics and Astronomy, Clemson University, Clemson, SC. 2Geophysical Institute, University of Alaska Fairbanks, Fairbanks, AK

Abstract: Since the early 1990's, a number of chemical tracer wind measurements have been carried out with sounding rockets launched from the Poker Flat Research Range in Alaska. The measurements cover a range of activity levels. Most of the measurements were made near local magnetic midnight or in the post midnight sector, although a few pre-midnight measurements are also available. The poster focuses on the winds observed in the lower E region in the altitude range between 90 and 120 km and discusses the features that are common in the wind profiles and the differences observed for different activity levels.

MLTS-07 Planning and simulating observations for a sounding rocket experiment measuring thermospheric nitric oxide(NO) in the polar night by stellar occultation - by Padma Thirukoveluri

Status of First Author: Student NOT in poster competition PhD

Authors: Padma Thirukoveluri, Virginia Tech, Scott M.Bailey, Virginia Tech, William E.McClintock, University of Colorado.

Abstract: We describe a sounding rocket experiment in development for launch in 2011. It will observe stars in occultation to measure thermospheric nitric oxide (NO) for the first time in the polar night. The observations are made at 215nm. NO is created in the polar night through precipitating energetic electrons and their secondaries. It has been postulated that NO transported to lower altitudes leads to significant ozone destruction. We will discuss the experiment and planning including the star selection process, viewing geometry including rocket-star, rocket-sun and rocket-moon zenith angle requirements and occultation altitudes, and other issues such as timing constraints for the launch. Some simulation results will be presented which are used to plan the measurement process.

MLTS-08 Gravity wave impacts on the atmospheric coupling from the MLT region to the stratosphere during stratospheric sudden warming with TIME-GCM - by Chihoko Yamashita

Status of First Author: Student IN poster competition PhD

Authors: Chihoko Yamashita (University of Colorado, NCAR/HAO), Han-Li Liu (NCAR/HAO), Xinzhao Chu (University of Colorado, CIRES)

Abstract: The stratospheric sudden warming (SSW) is a dramatic event with the sudden increase of temperature and wind reversal. Although SSWs only occur in winter stratosphere, SSWs have significant impacts on global atmospheric circulation from the troposphere to the thermosphere. The SSWs is the great example to understand the atmospheric coupling. TIME-GCM captured the general features of SSWs; however, the discrepancies between simulations and SABER observations still exist. These discrepancies lie in two major categories: (1) the locations and depth of cooling and warming regions in MLT, and (2) the downward progression of temperature anomaly from the mesosphere to the stratosphere. Both discrepancies may be due to unrealistic gravity wave parameters in TIME-GCM. Mesospheric cooling and lower thermospheric warming during SSWs are believed to result from the changes in the gravity wave transmission. For the downward propagation of temperature anomaly, we hypothesize that the gravity waves may play an important role in it through influencing the height of the zero-wind line that is the critical layer for the stationary planetary waves. In this study, the gravity wave roles in two discrepancies are investigated with the TIME-GCM through varying the gravity wave parameters in the model.

MLTS-09 Baroclinic Conditions and Anomalous Temperature Excursions of the Arctic Winter Middle Atmosphere: Discovery of Separated Mesopauses - by Katelynn Greer

Status of First Author: Student IN poster competition PhD

Authors: Katelynn Greer, Dr. Jeffrey Thayer: jeffrey.thayer@colorado.edu, Dr. Lynn Harvey: lynn.harvey@lasp.colorado.edu

Abstract: A separated mesopause at an altitude near 75 km is discovered (in addition to the nominal winter mesopause) that is associated with Stratopause Warming and Mesospheric Cooling (SWMC) events, which may be a precondition for

Sudden Stratospheric Warmings. The strongly baroclinic conditions at the stratopause, strikingly similar to frontal behavior, imply large vertical air motions reaching deep into the mesosphere and evidenced by the separated mesopause.

MLTS-10 Correlation of Mesospheric Polar Cloud Observational Data for the Northern Hemisphere in 2007 - by Jaimy Nicholle Tomlinson

Status of First Author: Student IN poster competition Undergraduate

Authors: Jaimy Tomlinson, Jodie Tvednes, Mike Taylor (CASS, Utah State University); Matt Deland (Science Systems and Applications Inc., Maryland); Mark Zalcik (Edmonton, Canada)

Abstract: Noctilucent clouds occur in the cold (<150 K) summer mesosphere at high latitudes. They stand out brightly against a dark twilight sky because they are high enough that the sun still illuminates them when it is $\sim 5^\circ$ to 16° below the horizon. These clouds are known as polar mesospheric clouds (PMCs) when observed from space. Satellites use back-scattering methods to measure the ultraviolet light scattered from the microscopic ice particles that make up these clouds. PMCs appear as enhancements in the back-scattering intensity. Algorithms are applied to the satellite data to separate the measurement of light scattered by PMCs from the background scattering by the rest of the atmosphere. The resulting data is analyzed to find latitudinal extent and patterns of occurrence frequency that might help us achieve a better understanding of the mesosphere and changes that may have occurred in the upper atmosphere over the last few decades. Some scientists propose that the occurrence frequency and brightness of PMCs have increased over the past century, and that this may be indicative of global climate change. Solar Backscatter Ultraviolet (SBUV) instruments on the NOAA satellite series provide continuous PMC data for the past 30 years. In conjunction with these observations, we are currently studying data from the new Ozone Monitoring Instrument (OMI) on the AURA satellite. In this poster, we compare 2007 northern hemisphere season OMI data with SBUV data and coincident ground-based observations from the Canadian CanAm observing network. We have identified several days during the 2007 season with OMI detections coinciding in time and space with visual observations reported by CanAm.

Bageston, José, 15
Bass, Elizabeth, 1

Carlson, Chad, 10
Chandran, Amal, 11
Chang, Loren, 16
Cheung, Elim, 1

de Larquier, Sebastien, 19
Drob, Douglas, 5

Fentzke, Jonathan, 20
Fernandez, Jose, 19
Friedman, Jonathan, 16

Greer, Katelynn, 21

Han, Feng, 4
Harrell, Sean, 5
Hayman, Matthew, 6
Huang, Wentao, 7

Irving, Brita, 9

Kafle, Durga, 11
Kim, Jung Soo, 17

Li, Jingbo, 2
Li, Tao, 12
Li, Zhenhua, 20
Lu, Gaopeng, 3
Lu, Xian, 16

Mangogna, Tony, 7
Marshall, Robert, 4

Patel, Pruthvish, 18
Paulino, Igo, 15
Petersen, Lance, 2
Pugmire, Jonathan, 12

Riousset, Jeremy, 3

Santos, Pedrina, 19
Scott, Tyler, 20
She, Chiao-Yao, 8
Simkhada, Deepak, 13
Slanger, Tom, 6
Smith, Camille, 13
Smith, John, 8
Snively, Jonathan, 15
Sparks, Jonathan, 1
Stockwell, Bob, 18

Taylor, Mike, 2
Thacker-Dey, Robert, 14
Thirukoveluri, Padma, 21
Thurairajah, Brentha, 9
Tomlinson, Jaimy, 22

Varney, Roger, 14
Vaudrin, Cody, 7

Wang, Zhangjun, 7
Watchorn, Steven, 6
Wu, Qian, 13

Xue, Xianghui, 9

Yamashita, Chihoko, 21
Yuan, Tao, 17
Yue, Jia, 9

Zhu, Xun, 14